Supporting Information: The C(^{3}P) + O$_2$($^3\Sigma_g^-$) $\leftrightarrow$ CO$_2$ $\leftrightarrow$ CO($^1\Sigma^+$)+ O(^{1}D)/O(^{3}P) Reaction: Thermal and Vibrational Relaxation Rates from 15 K to 20000 K

Juan Carlos San Vicente Veliz,[†] Debasish Koner,[†,¶] Max Schwilk,[†,§] Raymond J. Bemish,[‡] and Markus Meuwly[*,†,‖]

†*Department of Chemistry, University of Basel, Klingelbergstrasse 80, CH-4056 Basel, Switzerland*

‡*Air Force Research Laboratory, Space Vehicles Directorate, Kirtland AFB, New Mexico 87117, USA*

¶*Present Address: Department of Chemistry, Indian Institute of Science Education and Research (IISER) Tirupati, Karakambadi Road, Mangalam, Tirupati 517507, Andhra Pradesh, India*

§*University of Vienna, Faculty of Physics, 1090 Vienna, Austria*

E-mail: m.meuwly@unibas.ch

April 8, 2021

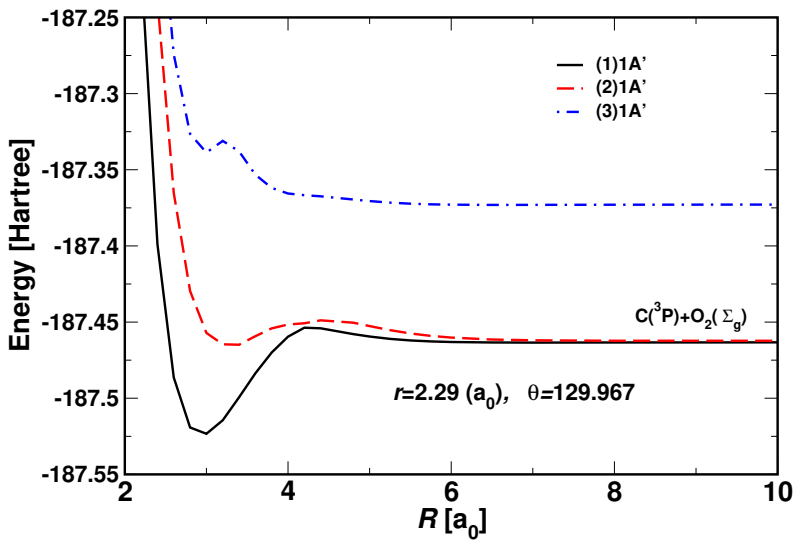

[b]

Figure S1: Dissociation curves for $C(^3P) + O_2(^3\Sigma_g)$ at $r_{O-O} = 2.29$ a_0 and $\theta = 129.95°$ with varying R. Calculations at SA-CASSCF level with 3 considered states of the singlet $^1A'$ state.

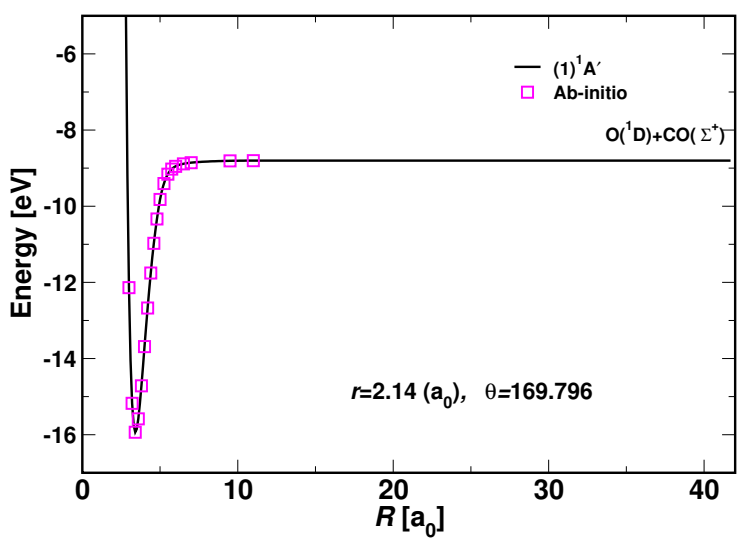

[b]

Figure S2: One-dimensional cut through the $^1A'$ PES illustrating the long-range behaviour of the RKHS representation (solid line) compared with the reference energies (open squares). Trajectories are started at $R = 19$ a_0.

References

(1) Jaffe, S.; Klein, F. S. Isotopic exchange reactions of atomic oxygen produced by the photolysis of NO_2 at 3660 Å. *Trans. Faraday Soc.* **1966**, *62*, 3135–3141.

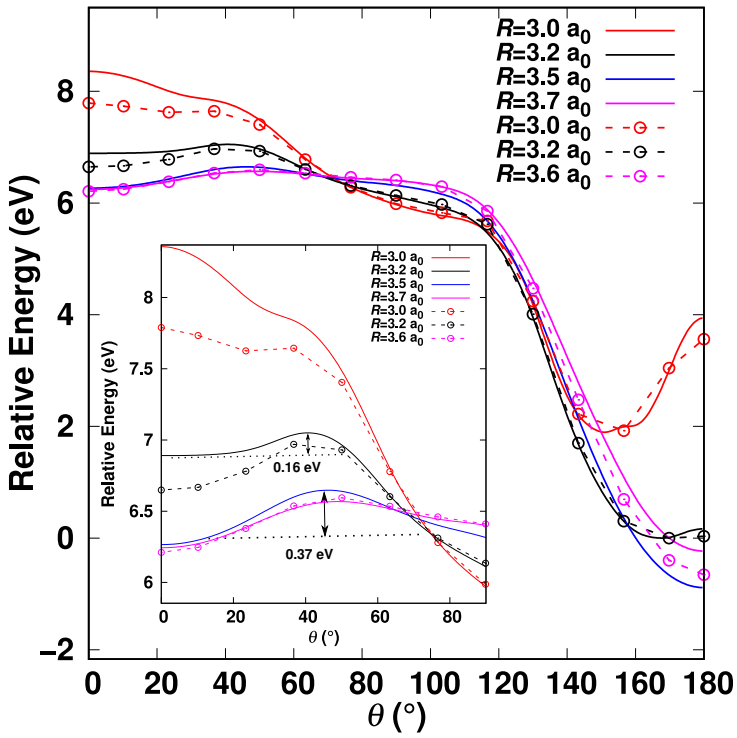

Figure S3: Angular cuts through the ^{1}A′ MRCISD-PES (red) and CCSD(T) (black) for different values of R. At both levels of theory the COO structure is found to be a local minimum, stabilized by ~ 9 (MRCISD) and ~ 5 kcal/mol (0.39 and 0.22 eV) (CCSD(T)), respectively. The energy of the COO conformation lies 170 kcal/mol (7.37 eV) above the global minimum. The zero of energy is the minimum for $R = 3.2$ a$_0$ for both the MRCISD-RKHS (solid lines) and *ab-initio* CCSD(T) (open circles and dashed lines), using the aug-cc-pVTZ basis set in both calculations.

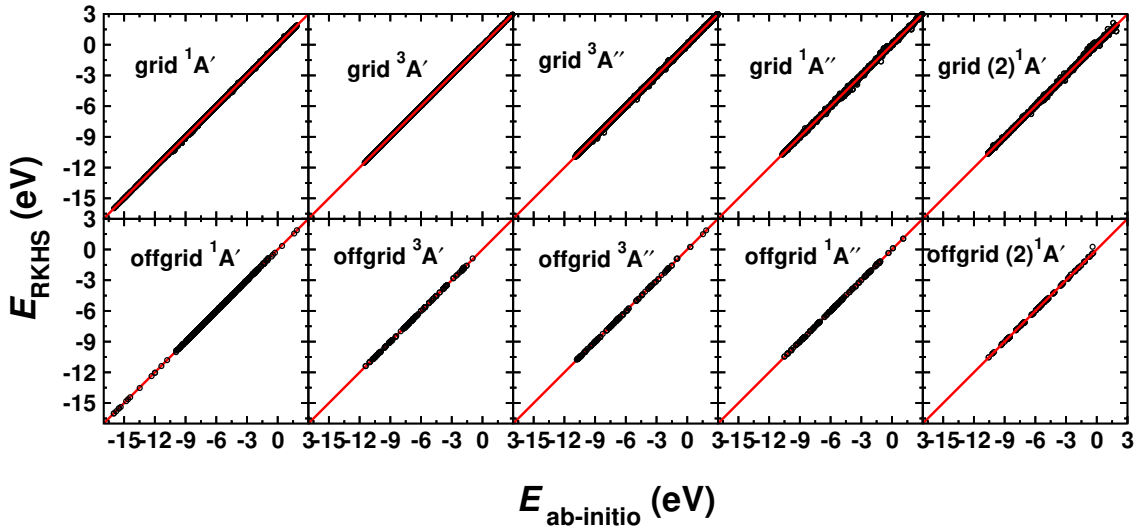

Figure S4: Correlation between MRCISD/aug-cc-PVTZ ($x-$axis) and RKHS energies ($y-$axis) for 23230 (^{1}A′), 9114 (^{3}A′), 20076 (^{3}A″), 19560 (^{1}A″), and 20696 ((2)^{1}A′) for grid points and 618, 201, 194, 188 and 134 offgrid points for the ^{1}A′,^{3}A′, ^{3}A″, ^{1}A″, and (2)^{1}A′ surfaces, respectively. The zero of energy is the O+O+C dissociation limit. The R^2 value for the grid points are (0.99998, 0.99999, 0.99996,0.99984, 0.99984) and for off-grid points (0.99993, 0.99991, 0.99990,0.99991, 0.99941) for the (^{1}A′,^{3}A′, ^{3}A″,^{1}A″) surfaces, respectively. The corresponding root mean squared errors (RMSE) for the ^{1}A′,^{3}A′, ^{3}A″, ^{1}A″ and (2)^{1}A′ surfaces are (0.01, 0.01, 0.02, 0.05, 0.04) eV (0.33, 0.27, 0.56, 1.04, 0.81) kcal/mol for the grid points and (0.03, 0.03, 0.04, 0.03, 0.03) eV (0.65, 0.72, 0.89, 0.59, 0.75) kcal/mol for offgrid points.

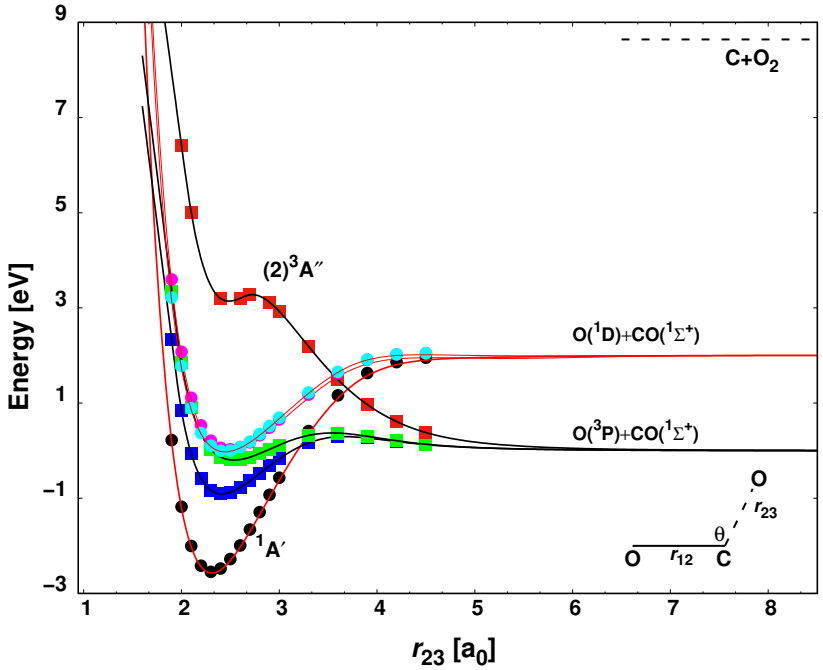

Figure S5: Ab initio calculated (points) and RKHS energies (solid lines) at a fixed CO bond length 1.2 Å (2.267 eV)and OCO angle $\theta = 120.0°$ for the ^{1}A′ (black solid circle), 2^1A′ (cyan solid circle), ^{1}A″ (magenta solid circle), ^{3}A′ (blue solid square), ^{3}A″ (green solid square), 2^3A″ (red solid square).

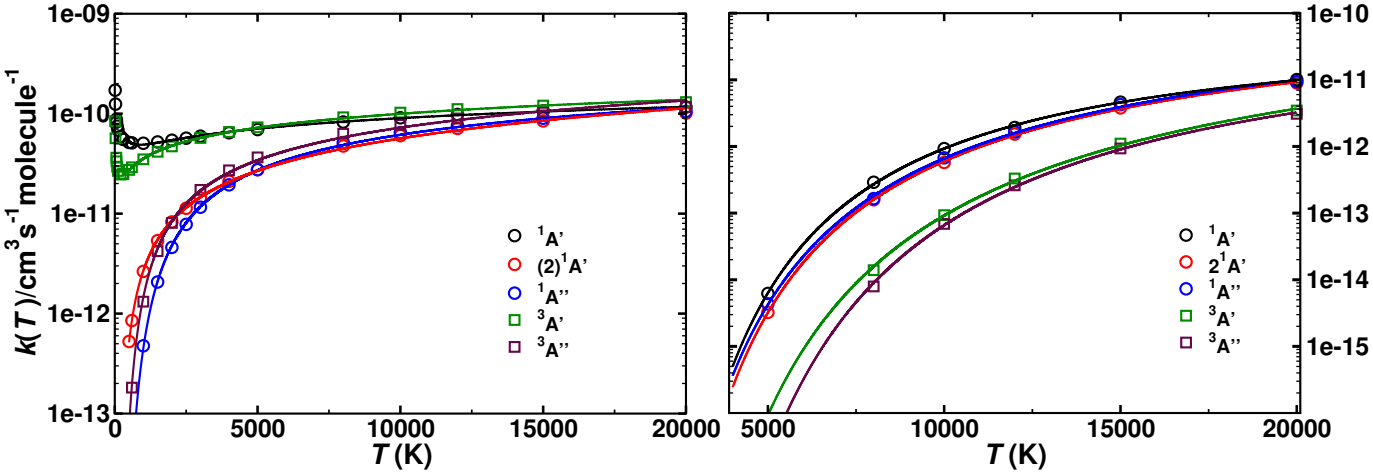

Figure S6: Rates for the forward (left) and reverse (right) reactions involving all five PESs. Symbols are the QCT results and solid lines are the fits to the modified Arrhenius equation. Circles for the rates on the singlet PESs and squares for those on the triplet PESs. Note the different scales along the $y-$axis for the forward and reverse rates.

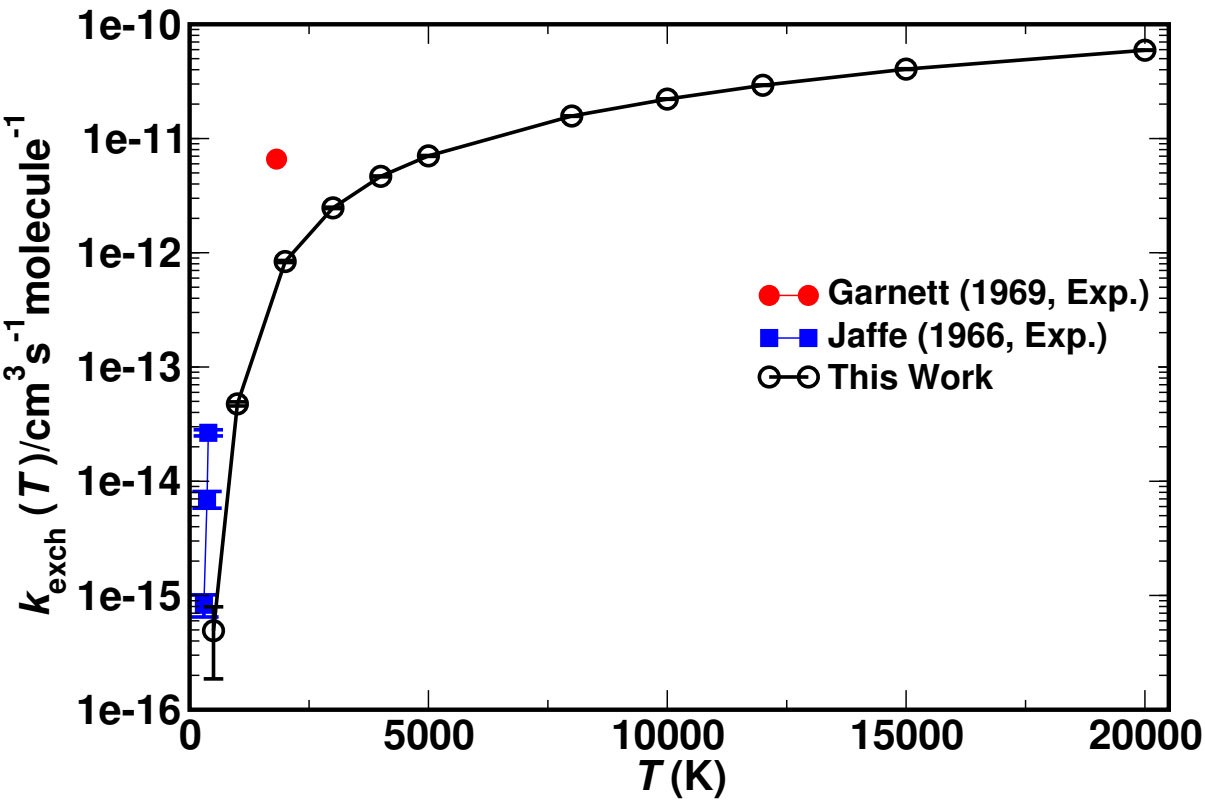

Figure S7: Comparison of computed and experimentally observed[1,2] rates for the $CO_A(^1\Sigma^+)$+ $O_B(^3P) \rightarrow CO_B(^1\Sigma^+)$+ $O_A(^3P)$ exchange reaction. At low temperatures[1] the computations are in better agreement with experiment than for the only high-temperature measurement.[2]

(2) Garnett, S. H.; Kistiakowsky, G. B.; O Grady, B. V. Isotopic Exchange between Oxygen and Carbon Monoxide in Shock Waves. *J. Chem. Phys.* **1969**, *51*, 84–91.

(3) Costes, M.; Naulin, C. State-to-state cross sections for the $C(^3P_J)$+ $O_2(X^3\Sigma_g^-) \rightarrow CO(X^1\Sigma^+)$+ $O(^1D_2)$ reaction at kinetic energies between 4.4 and 90 meV. *Comptes Rendus de l'Académie des Sciences-Series IIC-Chemistry* **1998**, *1*, 771–775.

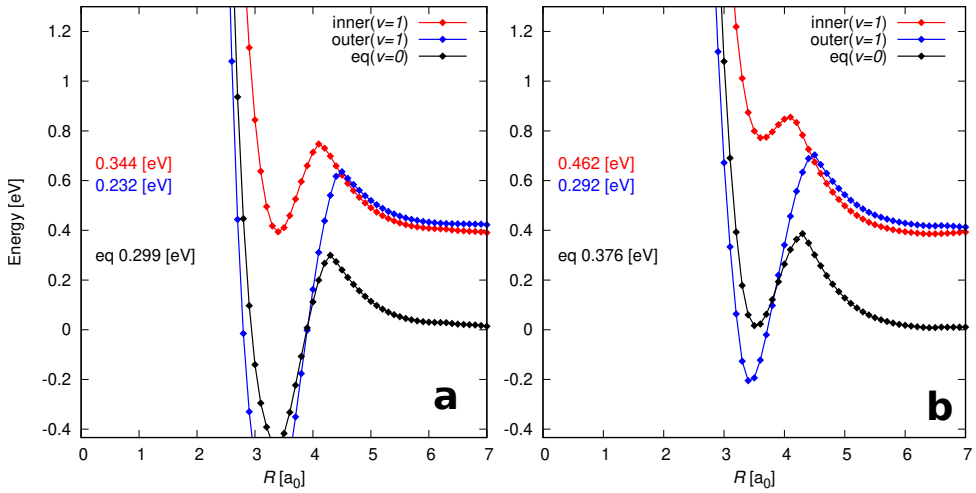

Figure S8: One-dimensional potential energy curves for the $CO_A(^1\Sigma^+) + O_B(^3P) \rightarrow CO_B(^1\Sigma^+) + O_A(^3P)$ atom exchange reaction on the $^3A'$ (left) and $^3A''$ PESs. The curves are drawn for fixed CO bond length at the equilibrium (black), ($v = 1$) inner (red), and ($v = 1$) outer (blue) turning points. For both electronic states the barrier height experienced by the approaching oxygen atom O_B depends on the separation of the CO_A diatom.

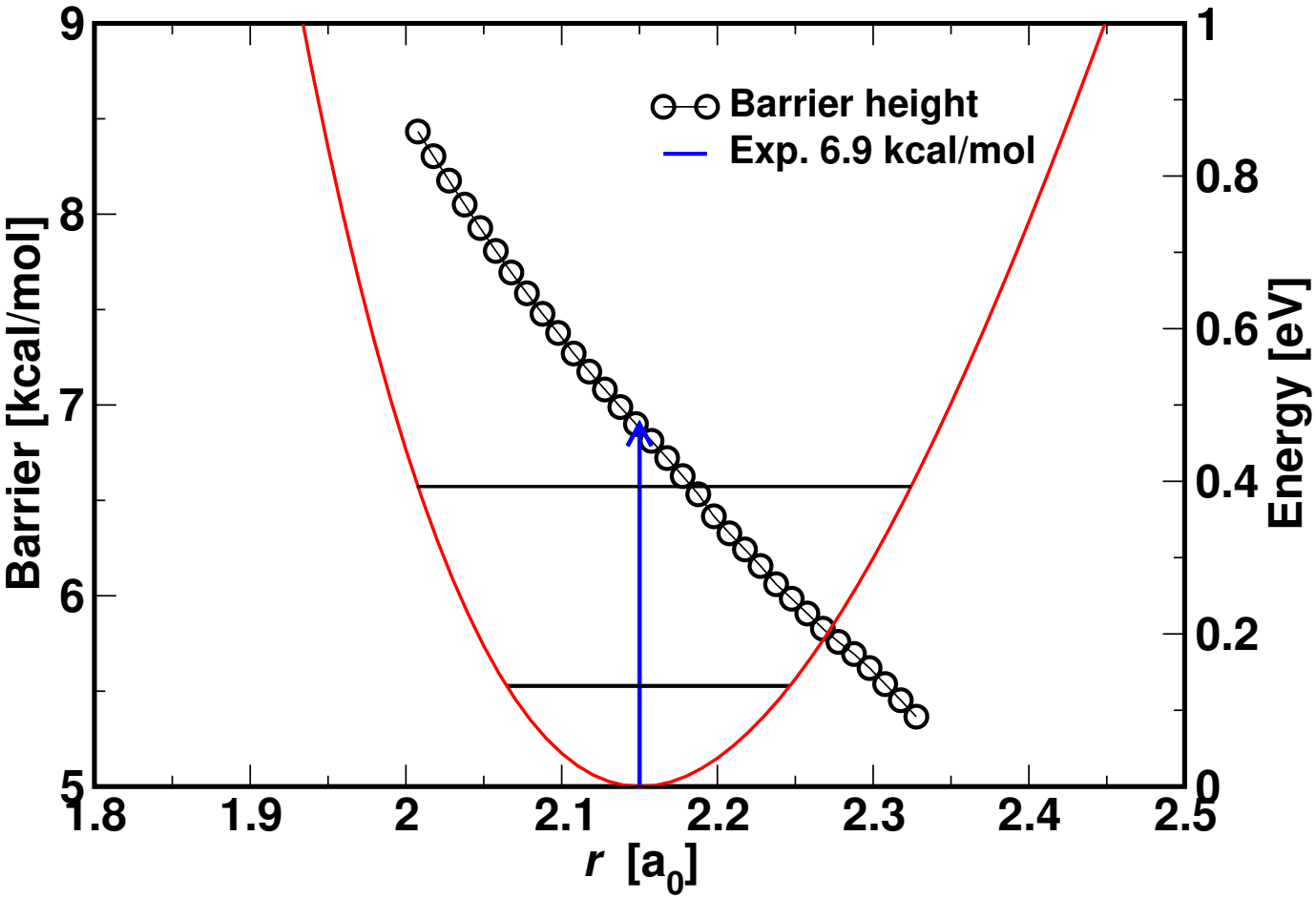

Figure S9: The barrier for the $CO_A(^1\Sigma^+) + O_B(^3P) \rightarrow CO_B(^1\Sigma^+) + O_A(^3P)$ atom exchange reaction on the $^3A'$ PES evaluated for CO separations between the inner and outer turning points for $v_{CO} = 1$. The CO potential with the $v = 0$ and $v = 1$ state is superimposed. The figure clarifies that the barrier towards formation of CO_2 varies between 8.5 kcal/mol (0.369 eV) and 5.5 kcal/mol (0.239 eV) at the inner and outer $v = 1$ turning points. Hence, the CO vibration acts as a gating mode. The barrier height for the isotopic exchange reaction at 300 K was reported[1] to be 6.9 kcal/mol (0.299 eV), consistent with the barriers found here.

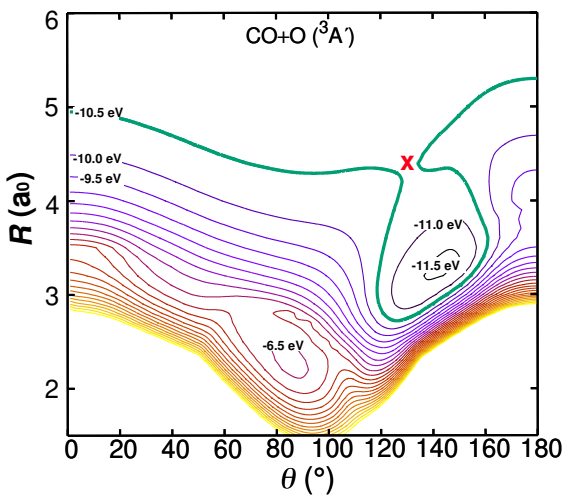

Figure S10: Relaxed 2D-PES for the CO + O asymptote for the ^{3}A′ state. The diatomic distance r ranges from 2.1 a_0 to 3.0 a_0. Contour lines are separated by 0.5 eV between 0 and –11.5 eV with the C+O+O dissociation energy as the zero of energy. The solid green line represents the –10.5 eV isocontour as a reference. It is noted that the relaxing and reactive trajectories leave the strongly interacting region through the opening, indicated by the red cross, around $R \sim 4.0$ a_0 and $\theta = 130°$.

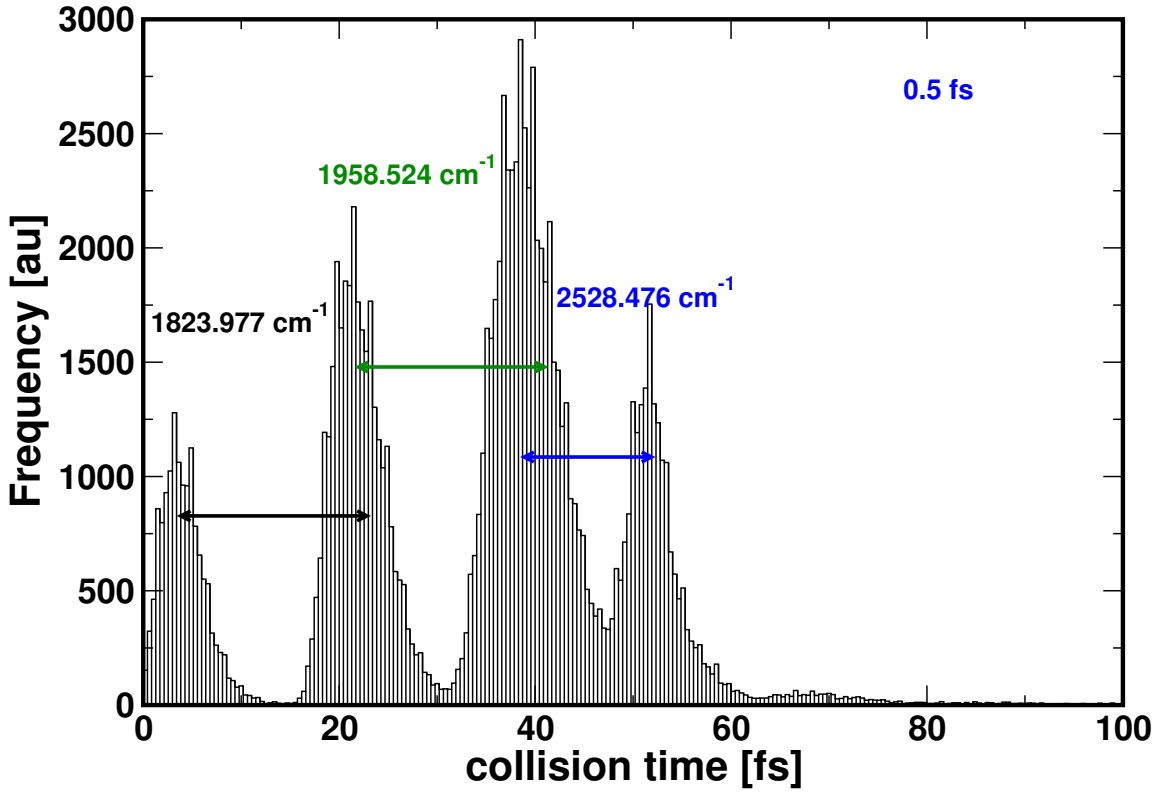

Figure S11: Collision time histogram for $\nu = 1$. Difference between adjacent peaks are displayed in cm^{-1}

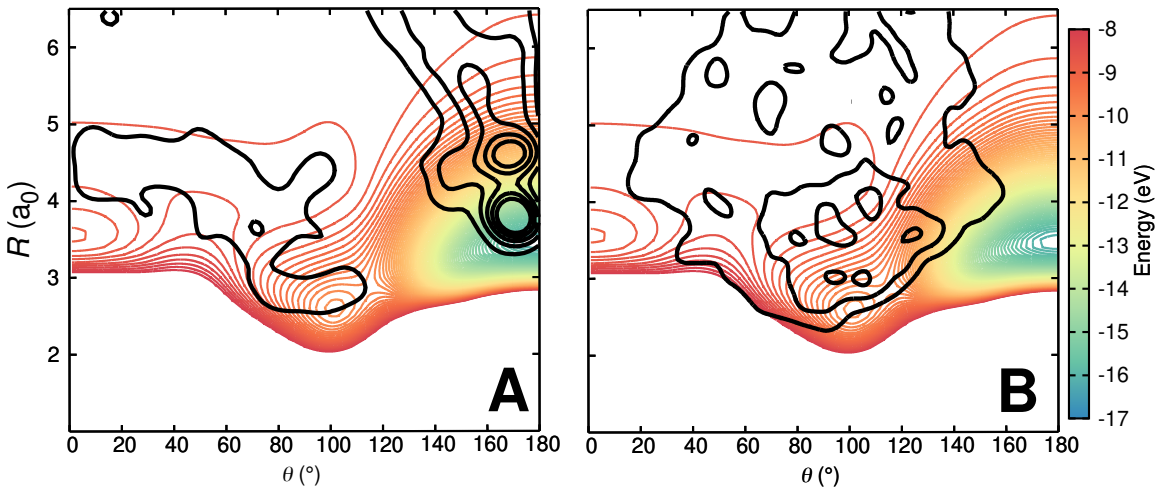

Figure S12: Density trajectory map at 15 K (panel A) and 10000 K (panel B) for the C+O_2 $\longrightarrow$ CO+O(^{1}D) reactive collisions on the ground state ^{1}A$'$ PES. The density map for the trajectories is superimposed on a relaxed 2D RKHS PES where $2.00 < r < 2.30$ a_0 (turning points). 300 reacting trajectories were taken for each case and represented as a KDE. It is found that although both sets of trajectories describe the same physical process (atom exchange reaction) they are sensitive to and sample different parts of the PES.

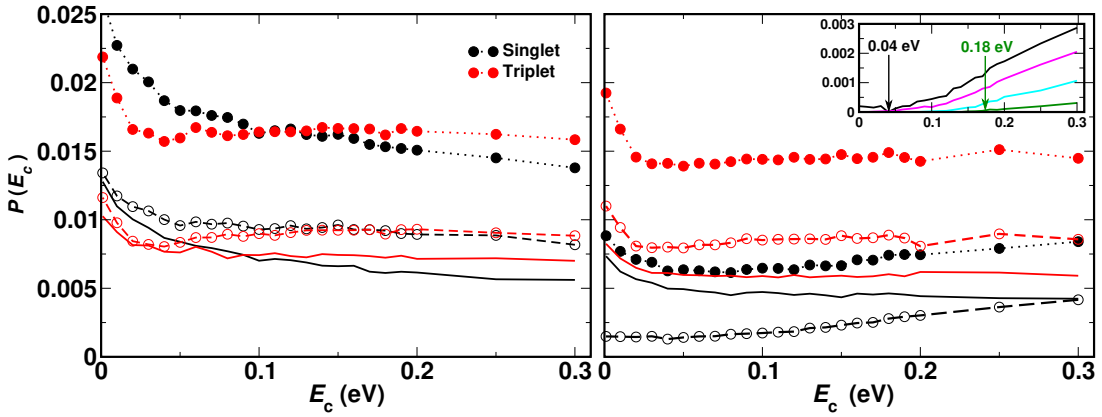

Figure S13: Reaction probability $P(E_c)$ as a function of collision energy E_c for the C(^{3}P) + O_2($^3\Sigma_g^-$) $\longrightarrow$ CO($^1\Sigma^+$) + O(^{1}D) (singlet (black), ^{1}A$'$ PES) and C(^{3}P) + O_2($^3\Sigma_g^-$) $\longrightarrow$ CO($^1\Sigma^+$) + O(^{3}P) (triplet (red), ^{3}A$'$ PES) reaction. Left panel for final vibrational state CO ($v' = 16$) and right panel for CO($v' = 17$). At least 10^5 trajectories were run for each collision energy (0.001-0.300 eV). Filled circles: total reaction probability; open circles: reaction probability originating from $O_2(v = 0)$; solid line: reaction probability originating from $O_2(v > 0)$. The inset in the right hand panel shows an enlargement for the singlet channel (forming O(^{1}D)) and highlights the threshold energy observed from experiment[3] to open this product channel at $E_c = 0.04$ eV. The green, cyan, magenta, and black traces correspond to initial $O_2(v = 0, j_{\max} < 10)$, $O_2(v = 0, j_{\max} < 20)$, $O_2(v = 0, j_{\max} < 30)$, and $O_2(v = 0)$ for all $j-$values.

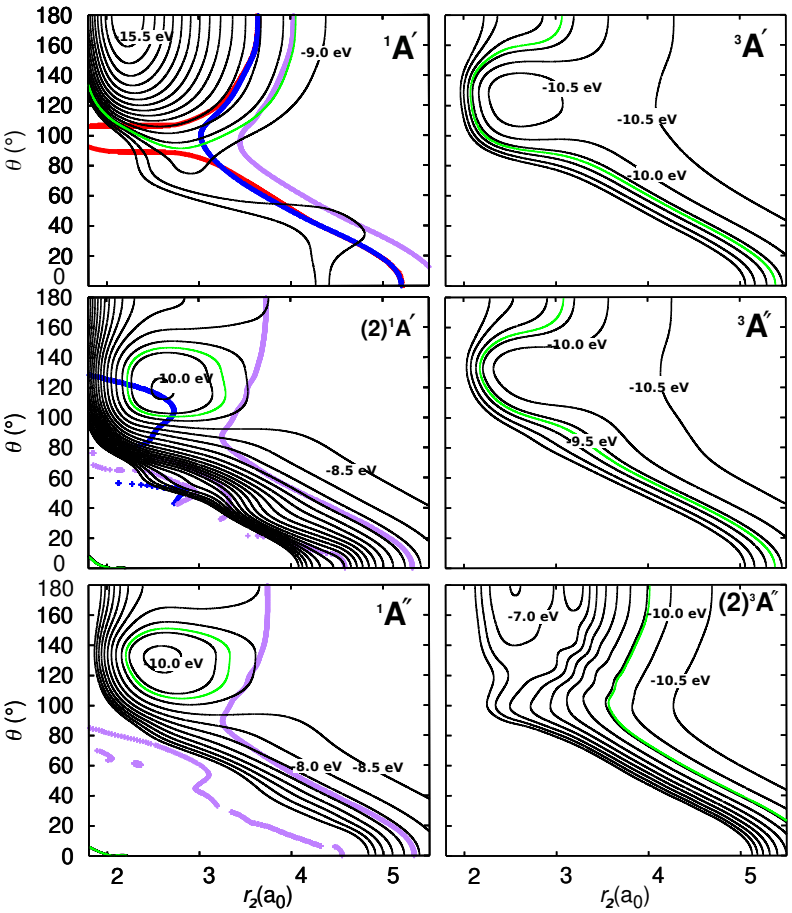

Figure S14: Crossings between the singlet and triplet PESs at the inner turning point (r_1 = 2.06 a$_0$) of the CO diatom. The distance r_2 is the second CO distance. Contour representation of the singlet (left) and triplet (right) states. Colour lines represent the intersection seam between the singlet and respective triplet surfaces. ^{1}X–^{3}A′ (red), ^{1}X–^{3}A″ (blue) and ^{1}X–(2)^{3}A″ (magenta). Green line indicates a reference contour at –9.5 eV relative to the O+O+C dissociation.

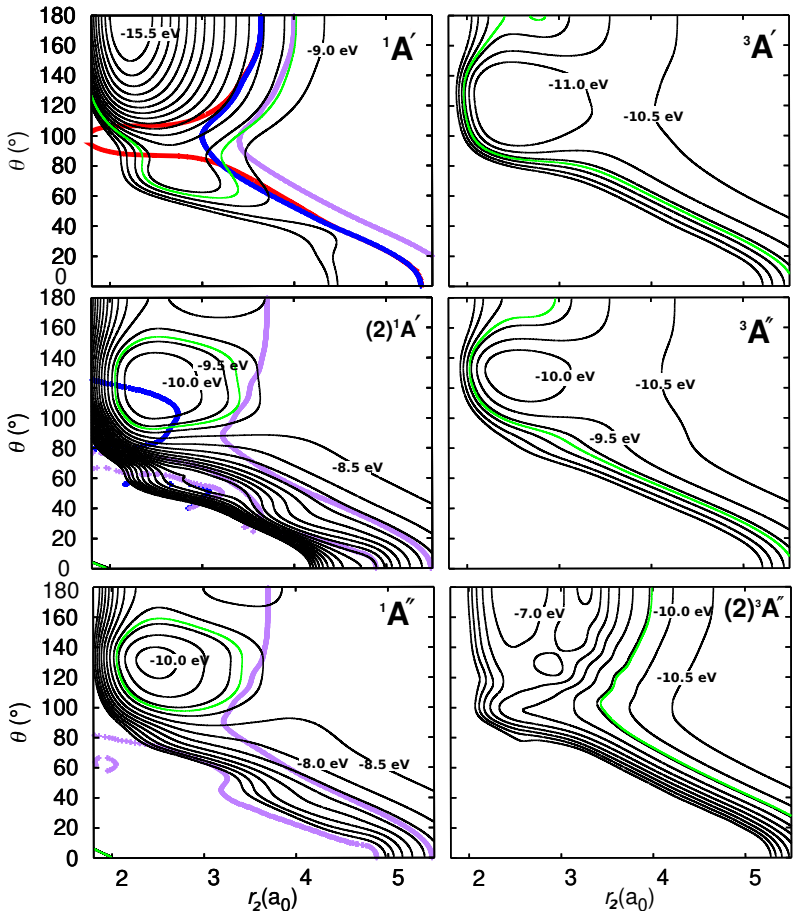

Figure S15: Crossings between the PESs at the outer turning point (r = 2.24 a$_0$) of the CO diatom. The distance r_2 is the second CO distance. Contour representation of the singlet (left) and triplet (right) states. Colour lines represent the intersection seam between the singlet and respective triplet surfaces. ^{1}X–^{3}A′ (red), ^{1}X–^{3}A″ (blue) and ^{1}X–(2)^{3}A″ (magenta). Green line indicates a reference contour at –9.5 eV relative to the O+O+C dissociation.

Table S1: Rates for the $C(^3P) + O_2(^3\Sigma_g^-) \rightarrow CO(^1\Sigma^+) + O(^1D_2)$ from 15 to 20000 K calculated using QCT on the $^1A'$, $(2)^1A'$, $^1A''$ PESs. Units for rates are in $cm^3s^{-1}molecule^{-1}$. N_r is the number of reacting trajectories.

T (K)	N_r	$k_1^f(^1A')$	$k_2^f((2)^1A')$	$k_3^f(^1A'')$	$k_1^f(^1A') + k_2^f((2)^1A') + k_3^f(^1A'')$
15	93057	1.718×10^{-10}	0.000	0.000	1.718×10^{-10}
27	90583	1.245×10^{-10}	0.000	0.000	1.245×10^{-10}
54	85791	8.778×10^{-11}	0.000	0.000	8.778×10^{-11}
63	84463	8.261×10^{-11}	0.000	0.000	8.261×10^{-11}
83	81512	7.501×10^{-11}	0.000	0.000	7.501×10^{-11}
112	77896	6.868×10^{-11}	2.617×10^{-17}	0.000	6.868×10^{-11}
207	68861	5.925×10^{-11}	1.186×10^{-14}	0.000	5.926×10^{-11}
295	66814	5.551×10^{-11}	7.371×10^{-14}	2.095×10^{-16}	5.558×10^{-11}
300	66493	5.532×10^{-11}	7.785×10^{-14}	2.108×10^{-16}	5.540×10^{-11}
500	58788	5.152×10^{-11}	5.265×10^{-13}	6.183×10^{-15}	5.205×10^{-11}
600	56358	5.104×10^{-11}	8.512×10^{-13}	2.394×10^{-14}	5.191×10^{-11}
1000	53536	5.057×10^{-11}	2.643×10^{-12}	4.761×10^{-13}	5.369×10^{-11}
1500	49748	5.217×10^{-11}	5.368×10^{-12}	2.070×10^{-12}	5.961×10^{-11}
2000	50708	5.421×10^{-11}	8.266×10^{-12}	4.592×10^{-12}	6.707×10^{-11}
2500	49341	5.686×10^{-11}	1.132×10^{-11}	7.810×10^{-12}	7.599×10^{-11}
3000	48425	5.955×10^{-11}	1.434×10^{-11}	1.159×10^{-11}	8.549×10^{-11}
4000	46964	6.442×10^{-11}	2.102×10^{-11}	1.942×10^{-11}	1.049×10^{-10}
5000	46270	6.939×10^{-11}	2.752×10^{-11}	2.757×10^{-11}	1.245×10^{-10}
8000	52737	8.250×10^{-11}	4.748×10^{-11}	5.138×10^{-11}	1.814×10^{-10}
10000	52363	9.090×10^{-11}	6.025×10^{-11}	6.469×10^{-11}	2.158×10^{-10}
12000	51930	9.818×10^{-11}	7.120×10^{-11}	7.585×10^{-11}	2.452×10^{-10}
15000	50987	1.066×10^{-10}	8.462×10^{-11}	9.010×10^{-11}	2.813×10^{-10}
20000	49054	1.164×10^{-10}	1.013×10^{-10}	1.054×10^{-10}	3.232×10^{-10}

Table S2: Rate coefficients for the $C(^3P) + O_2(^3\Sigma_g^-) \rightarrow CO(^1\Sigma^+) + O(^3P)$ from 15 to 20000 K calculated using QCT on the $^3A'$ and $^3A''$ PESs. Units are in $cm^3s^{-1}molecule^{-1}$. N_r is the number of reacting trajectories.

T (K)	N_r	$k_1^f(^3A')$	$k_2^f(^3A'')$	$k_1^f(^3A') + k_2^f(^3A'')$
15	49736	8.414×10^{-11}	0.000	8.414×10^{-11}
27	47390	5.682×10^{-11}	0.000	5.682×10^{-11}
54	44900	3.632×10^{-11}	0.000	3.632×10^{-11}
63	44406	3.337×10^{-11}	0.000	3.337×10^{-11}
83	43644	2.949×10^{-11}	0.000	2.949×10^{-11}
112	43489	2.671×10^{-11}	0.000	2.671×10^{-11}
207	43238	2.460×10^{-11}	0.000	2.460×10^{-11}
295	46131	2.486×10^{-11}	1.467×10^{-15}	2.487×10^{-11}
300	46187	2.506×10^{-11}	1.476×10^{-15}	2.506×10^{-11}
500	46573	2.742×10^{-11}	8.043×10^{-14}	2.750×10^{-11}
600	46856	2.906×10^{-11}	1.818×10^{-13}	2.924×10^{-11}
1000	50249	3.498×10^{-11}	1.321×10^{-12}	3.630×10^{-11}
1500	50968	4.156×10^{-11}	4.213×10^{-12}	4.578×10^{-11}
2000	54396	4.706×10^{-11}	8.086×10^{-12}	5.514×10^{-11}
3000	54474	5.717×10^{-11}	1.729×10^{-11}	7.446×10^{-11}
4000	54387	6.554×10^{-11}	2.710×10^{-11}	9.264×10^{-11}
5000	54311	7.304×10^{-11}	3.655×10^{-11}	1.096×10^{-10}
8000	62916	9.208×10^{-11}	6.297×10^{-11}	1.551×10^{-10}
10000	62254	1.025×10^{-10}	7.745×10^{-11}	1.799×10^{-10}
12000	61260	1.113×10^{-10}	8.944×10^{-11}	2.007×10^{-10}
15000	59333	1.205×10^{-10}	1.027×10^{-10}	2.232×10^{-10}
20000	55854	1.306×10^{-10}	1.166×10^{-10}	2.472×10^{-10}

Table S3: Rate coefficients for the $CO(^1\Sigma^+) + O(^1D) \rightarrow C(^3P) + O_2(^3\Sigma_g^-)$ from 3000 to 20000 K calculated using QCT on the $^1A'$, $(2)^1A'$, $^1A''$ PESs. Units are in $cm^3s^{-1}molecule^{-1}$. N_r is the number of reacting trajectories.

T (K)	N_r	$k_1^r(^1A')$	$k_2^r((2)^1A')$	$k_3^r(^1A'')$	$k_1^r(^1A') + k_2^r((2)^1A') + k_3^r(^1A'')$
3000	0	0.000	0.000	0.000	0.000
4000	3	6.226×10^{-16}	3.738×10^{-16}	0.000	9.964×10^{-16}
5000	16	6.236×10^{-15}	3.239×10^{-15}	4.351×10^{-15}	1.383×10^{-14}
8000	383	2.902×10^{-13}	1.588×10^{-13}	1.651×10^{-13}	6.141×10^{-13}
10000	1037	9.278×10^{-13}	5.759×10^{-13}	6.744×10^{-13}	2.178×10^{-12}
12000	1897	1.928×10^{-12}	1.533×10^{-12}	1.653×10^{-12}	5.114×10^{-12}
15000	3711	4.616×10^{-12}	3.796×10^{-12}	4.239×10^{-12}	1.265×10^{-11}
20000	6655	1.008×10^{-11}	8.983×10^{-12}	9.373×10^{-12}	2.844×10^{-11}

Table S4: Rate coefficients for the $CO(^1\Sigma^+)$+ $O(^3P) \rightarrow C(^3P)$ + $O_2(^3\Sigma_g^-)$ from 3000 to 20000 K calculated using QCT on the $^3A'$ and $^3A''$ PESs. Units are in $cm^3s^{-1}molecule^{-1}$. N_r is the number of reacting trajectories.

T (K)	N_r	$k_1^r(^3A')$	$k_2^r(^3A'')$	$k_1^r(^3A') + k_2^r(^3A'')$
3000	0	0.000	0.000	0.000
4000	0	0.000	0.000	0.000
5000	2	9.055×10^{-17}	2.175×10^{-17}	1.123×10^{-16}
8000	223	1.429×10^{-14}	7.940×10^{-15}	2.223×10^{-14}
10000	1332	9.277×10^{-14}	6.892×10^{-14}	1.617×10^{-13}
12000	4339	3.340×10^{-13}	2.609×10^{-13}	5.948×10^{-13}
15000	11796	1.098×10^{-12}	9.348×10^{-13}	2.033×10^{-12}
20000	28176	3.449×10^{-12}	3.087×10^{-12}	6.535×10^{-12}

Table S5: Temperature dependent rates for the $CO_A(^1\Sigma^+)$+ $O_B(^3P) \rightarrow CO_B(^1\Sigma^+)$+ $O_A(^3P)$ exchange reaction from 500 to 20000 K calculated using QCT on the $^3A'$ PESs. Units are in $cm^3s^{-1}molecule^{-1}$. N_r is the number of reacting trajectories.

T (K)	N	$k_1^f(^3A')$	$k_1^f(^3A'')$	$k_1^f(^3A' +^3 A'')$	$\Delta k_1^f(^3A' +^3 A'')$
500	57	3.859×10^{-16}	1.053×10^{-16}	4.912×10^{-16}	3.052×10^{-16}
1000	425	3.511×10^{-14}	1.242×10^{-14}	4.754×10^{-14}	1.972×10^{-15}
2000	4734	5.570×10^{-13}	2.812×10^{-13}	8.382×10^{-13}	1.746×10^{-14}
3000	11621	1.503×10^{-12}	9.694×10^{-13}	2.472×10^{-12}	3.340×10^{-14}
4000	20393	2.649×10^{-12}	2.012×10^{-12}	4.661×10^{-12}	3.969×10^{-14}
5000	28143	3.808×10^{-12}	3.233×10^{-12}	7.041×10^{-12}	5.890×10^{-14}
8000	52280	7.947×10^{-12}	7.777×10^{-12}	1.572×10^{-11}	7.493×10^{-14}
10000	78807	1.116×10^{-11}	1.099×10^{-11}	2.215×10^{-11}	1.088×10^{-13}
12000	93891	1.459×10^{-11}	1.468×10^{-11}	2.927×10^{-11}	1.606×10^{-13}
15000	127016	2.008×10^{-11}	2.043×10^{-11}	4.051×10^{-11}	3.037×10^{-13}
20000	182669	2.932×10^{-11}	3.001×10^{-11}	5.933×10^{-11}	1.990×10^{-13}

Table S6: Rate coefficients for the CO($^1\Sigma^+$)+ O(^{3}P) $\rightarrow$ CO($^1\Sigma^+$)+ O(^{3}P) vibrational relaxation $\nu = 1 \rightarrow 0$ from 300 to 5000 K calculated using QCT on the ^{3}A$'$ and ^{3}A$''$ PESs and Gaussian binning. Units for rates are in cm^{3}s^{-1}molecule^{-1} and N_r is the number of reacting trajectories.

T (K)	N_r	$k_1^f(^3A')$	$k_1^f(^3A'')$	$k_1^f(^3A') + k_1^f(^3A'')$
300	0	0.000	0.000	0.000
500	6	8.475×10^{-16}	7.706×10^{-19}	8.483×10^{-16}
1000	172	1.289×10^{-13}	8.729×10^{-14}	2.162×10^{-13}
2000	1063	1.307×10^{-12}	8.973×10^{-13}	2.205×10^{-12}
3000	1948	2.926×10^{-12}	2.270×10^{-12}	5.206×10^{-12}
4000	2825	4.511×10^{-12}	4.387×10^{-12}	8.942×10^{-12}
5000	3333	5.881×10^{-12}	5.721×10^{-12}	1.178×10^{-11}